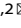## ARTICLE   OPEN

Check for updates

A temperature responsive adhesive hydrogel for fabrication of flexible electronic sensors

Wan Liu[1,2], Ruijie Xie[3], Jingyu Zhu[3], Jiansheng Wu[3], Junfeng Hui[1,2✉], Xiaoyan Zheng[2], Fengwei Huo [ID][3✉] and Daidi Fan[1,2✉]

Flexible electronics are playing an increasingly important role in human health monitoring and healthcare diagnosis. Strong adhesion on human tissue would be ideal for reducing interface resistance and motion artifacts, but arising problems such as skin irritation, rubefaction, and pain upon device removal have hampered their utility. Here, inspired by the temperature reversibility of hydrogen bonding, a skin-friendly conductive hydrogel with multiple-hydrogen bonds was designed by using biocompatible poly(vinyl alcohol) (PVA), phytic acid (PA), and gelatin (Gel). The obtained PVA/PA/Gel (PPG) hydrogel with temperature-triggered tunable mechanic could reliably adhere to skin and detect electrophysiological signals under a hot compress while be readily removed under a cool compress. Furthermore, the additional advantages of transparency, breathability, and antimicrobial activity of the PPG hydrogel ensure its long-time wearable value on the skin. It is both environmentally friendly and cost saving for the waste PPG hydrogel during production can be recycled based on their reversible physical bonding. The PPG hydrogel sensor is expected to have good application prospects to record electrophysiological signals in human health monitoring.

INTRODUCTION

Flexible electronics play important roles in human health monitoring and healthcare diagnosis by detecting a variety of vital signals, including physical signals (e.g., strain and motion) and electrophysiological signals (e.g., electrocardiogram (ECG), electroencephalography (EEG), and electromyogram (EMG) signals)[1–3]. Wearability is the key technology for the future development of flexible electronics[4]. Hydrogels, tissue-like softness yet achieving toughness and stretchability, are providing a platform for bioimplantable, tissue regeneration, and e-skin electronic devices[5]. Hydrogel-based ionic skins could reduce electron-ion interface resistance and motion artifacts to achieve more accurate detection result, paving the way for reciprocal information transmission between natural organisms and artificial devices[6–9]. However, the adhesion of such sensor usually fails to meet the requirement of practical applications. If its adhesion to skin is too weak, the sensor will shift arbitrarily during body movement, resulting in motion artifacts, noisy data, and subsequent misdiagnosis[10,11]. Whilst its strong adhesion to skin may cause inflammation, irritation, and pain to users upon removal[12,13]. Thus, it is desirable to design new-generation hydrogel-based skin adhesives to meet current needs.

To this end, many efforts on regulating adhesion between devices and skin have been reported[14–17]. Hydrogel adhesive is of interest because its adhesion can be tailored by modifying the chemical composition and surface groups with the help of complementary functional groups (carbon–carbon, carbon–nitrogen, siloxane, amide, and so on) and physical interactions (such as ionic bonds, hydrogen bonds, host–guest interactions, and van der Waals interactions)[18–20]. An effective strategy is to achieve on-demand detachable hydrogels by removing strong adhesion via detachment triggers[21]. For example, Guo et al. prepared a dual-dynamic-bond cross-linked hydrogel as a wound-healing dressing which could

achieve on-demand removal by the intervention of deferoxamine mesylate or acid solution[22]. Based on dynamic interactions, the hydrogel-based electronics-tissue interface has been reported recently and the interface could be detached by dissociating the dynamic complexes with adding glucose-trigger[23]. Problems, however, have been noted for using chemical reagent triggers. For one thing, the extra chemicals may cause skin damage; for another, the metabolites secreted by the skin can disguise as triggers, causing hydrogel separation and disfunction[24]. Physically induced detachable (near-infrared (NIR)[25], ultraviolet (UV)[26], and temperature[27]) hydrogels can avoid the issues and therefore capture much attention. Among them, temperature-controlled hydrogels are convenient for users because they can be triggered by the human body temperature without additional chemicals or devices. A temperature-triggered debonding-on-demand sticker was designed that could provide high adhesion flowability between 26 and 32 °C while be detached after cooling to temperature lower than 21 °C[27]. Inspired by the muscle actuation adhesion mechanism of octopus suckers, Wu et al. prepared a skin adhesive hydrogel patch with temperature trigger, featuring different skin anchoring strength at 20 and 37 °C[28]. As we know, the environmental temperature is often below 20 °C in winter and/or above 40 °C in summer, which means the adhesion of hydrogels is unstable in daily life and should be further improved. A popular trend of development is to devise a hydrogel adhesive with tunable mechanic.

Enlightened by the temperature reversibility of hydrogen bonding, biocompatible poly(vinyl alcohol) (PVA) and gelatin (Gel) have been employed to build a hydrogel network crosslinked with hydrogen bonds[29], and the phytic acid (PA) from plants was used to strengthen the PVA–Gel hydrogel network by forming multiple hydrogen bonds and act as a proton donor to increase hydrogel conductivity[30,31]. Herein, a facile strategy to fabricate a skin-friendly hydrogel with temperature-triggered adhesiveness

[1]Shaanxi Key Laboratory of Degradable Biomedical Materials, Shaanxi R&D Center of Biomaterials and Fermentation Engineering, School of Chemical and Engineering, Northwest University, Taibai North Road 229, Xi'an, Shaanxi 710069, China. [2]Biotech. & Biomed. Research Institute, Northwest University, Taibai North Road 229, Xi'an, Shaanxi 710069, China. [3]Key Laboratory of Flexible Electronics (KLOFE), Institute of Advanced Materials (IAM), Nanjing Tech University, 30 South Puzhu Road, Nanjing 211816, China. ✉email: huijunfeng@nwu.edu.cn; iamfwhuo@njtech.edu.cn; fandaidi@nwu.edu.cn

between 4 and 55 °C has been designed. Befitting from the reversibility of hydrogen and ionic bonds, PVA/PA/Gel (PPG) hydrogel could avoid damaging the skin during the peeling process. Specifically, the weak hydrogen bonds would be broken via a hot compress at approximately 55 °C to make the PPG hydrogel adhere and stay attached to the skin, to detect the electrophysiological signals during rest and movement with low motion artifacts. The obtained adhesiveness could be retained until a cool compress was applied to trigger hydrogen bond reforming. Such strategy allows the PPG hydrogel to be applied to monitor human health because it exhibits good transparency, self-adaptation, breathability, water retention, and antimicrobial activity. In addition, cross-linked by reversible ionic and hydrogen bonds, the waste PPG hydrogel during production could be recycled to reduce resource waste, production cost, and environmental pollution. Hence, the PPG hydrogel is expected to be valuable in the controllable adhesion of bioelectrodes for electrophysiological monitoring.

RESULTS AND DISCUSSION

Design and preparation of the PPG hydrogel

A facile two-step strategy was used to prepare the PPG hydrogel, as illustrated in Fig. 1a. First, raw materials (PVA, PA, and Gel) were dissolved in a glycerol-water binary solvent systems. The anchoring effect of glycerol on water molecules can reduce the stability of the hydration film around PVA and Gel molecules so that their molecular chains in the system can stretch and expose more groups to form intermolecular hydrogen bonds[32]. PA could form ionic bonds with the $-NH_2$ in Gel and hydrogen bonds with the $-OH$ in PVA, building an intermolecular stereoscopic network structure[33,34]. Secondly, the mixture was transferred into molds and placed at −20 °C for 24 h to obtain a sable hydrogel three-dimensional (3D) network structure. As shown in Supplementary Fig. 1, the PPG hydrogel obtained at 4 °C collapsed and exhibited weaker mechanical properties than that obtained at −20 °C. We found that low temperature is a decisive factor to form stronger and abundant hydrogen bonds, because the molecules move slowly at low temperature and have sufficient time to form hydrogen bonds. Thus, the resultant PPG hydrogel with abundant hydrogen bonds as shown in Fig. 1b is transparent and flexible enough to effectively adhere to knuckles.

Hydrogen bonding is a kind of physical interaction that is responsive to temperature. As shown in Fig. 1c, the response of PPG hydrogel was observed at different temperatures. The prepared PPG hydrogel remained almost unchanged when held at 37 °C for 5 min, whereas its viscosity increased significantly when preheated at 55 °C for 5 min and remained viscous when dropped back to 37 °C. More interestingly, the viscosity disappeared when the temperature was further dropped to 4 °C (around an ice pack temperature). Rheological properties were used to evaluate the viscoelasticity of the PPG hydrogel. When the
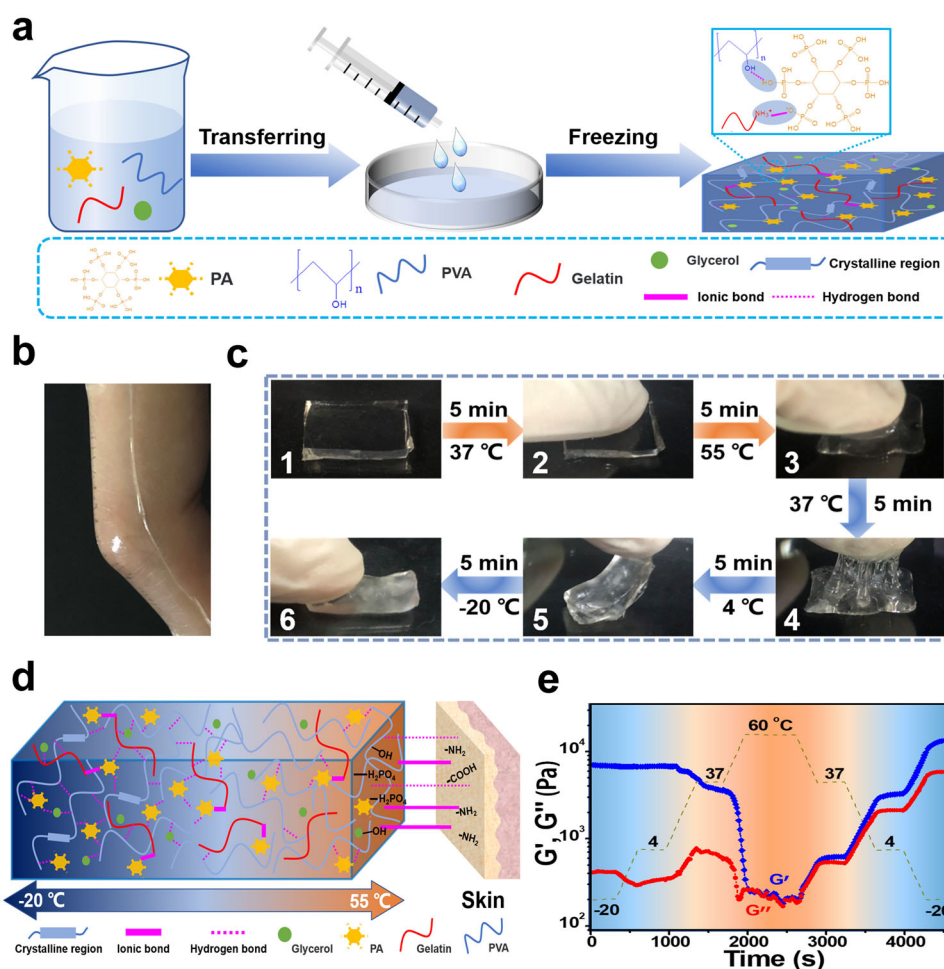

Fig. 1 Schematic illustration of the mechanism of PPG hydrogel. a Schematic illustration of the preparation about PPG hydrogel. **b** Photograph of the PPG hydrogel adhering to knuckles. **c** Photographs of the PPG hydrogel treated with different temperatures. **d** Schematic illustration of the mechanism about the controllable adhesion of the PPG hydrogel to skin. **e** Rheological properties of the PPG hydrogel at different temperatures.
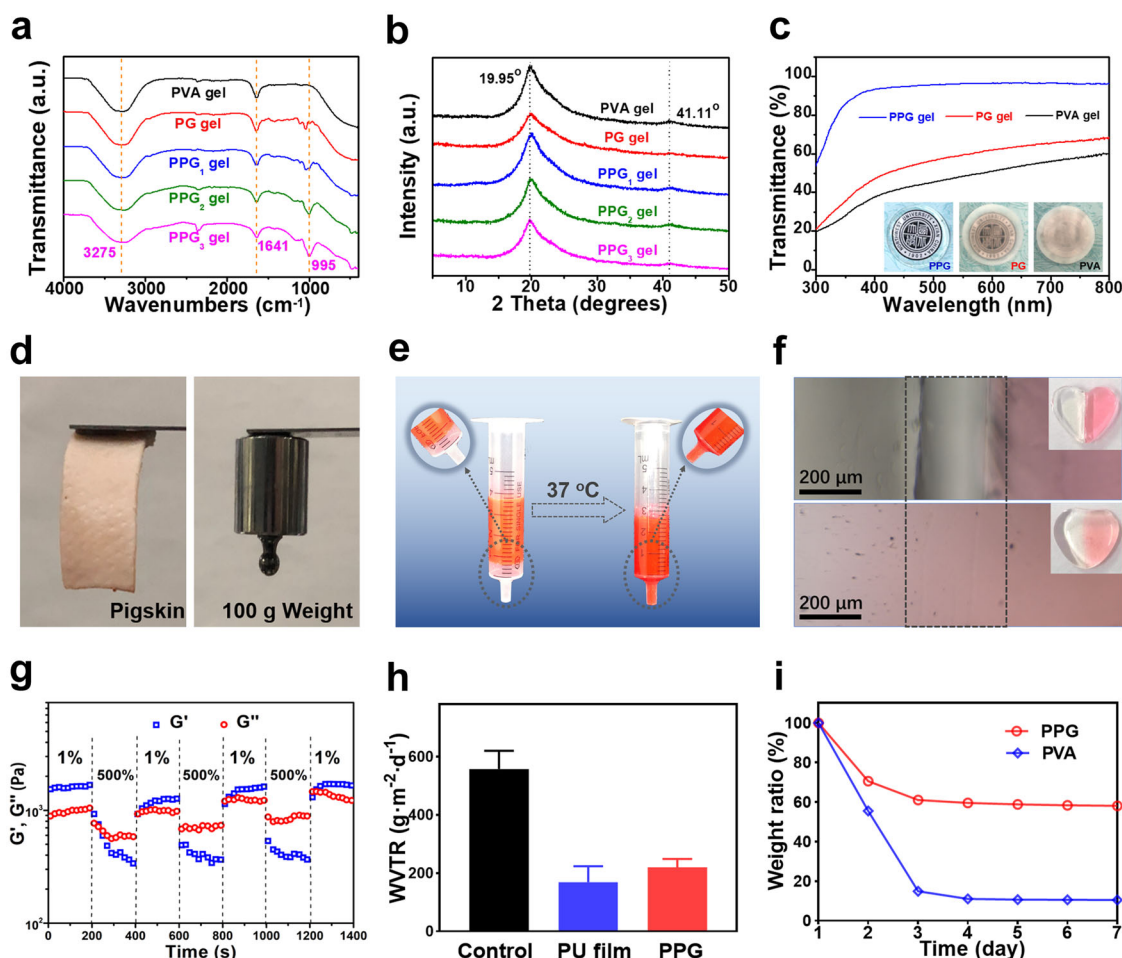
Fig. 2 Charcterization of PPG hydrogel. a FTIR spectra of the hydrogels. **b** XRD spectra of the hydrogels. **c** UV–vis spectra of hydrogels. Insert showing the optical transparency of the hydrogels. **d** Self-adhesion property of PPG hydrogel. **e** Self-adaptive property of PPG hydrogel marked with Rh B at 37 °C under gravity. **f** Optical microscope images of interface of the healed PPG hydrogel. Insert showing the healed PPG hydrogel. **g** Rheological property of PPG hydrogel at the alternate step strain test. **h** Breathability of PPG hydrogel and commercial PU film. Error bars represent the standard deviation ($n = 3$). **i** Weight losses of PVA and PPG hydrogels.

storage modulus (G') approaches to the loss modulus (G''), the hydrogel possesses gel–fluid dual properties. If $G' > G''$, the gel property is dominant; otherwise, the fluid property is dominant, and the gel state will collapse to a quasi-liquid state[35]. As shown in Fig. 1e, the PPG hydrogel exhibited a gel state ($G' > G''$) upon heating from −20 to 37 °C, while showcasing the dual properties ($G' ≈ G''$) after continuously heating to 60 °C. Finally, the gel states were restored step by step upon cooling to 37, 4, and −20 °C. This phenomenon shows that the PPG hydrogel possesses good temperature–responsive viscosity and may advance the temperature-responsive hydrogel adhesives. Figure 1d clearly depicted the controllable adhesion mechanism of the PPG hydrogel to skin. In a warm environment, weak hydrogen bond interactions will break and release the groups (–H_2PO_4 and –OH) that activate and form ionic and hydrogen bonds with the amino and carboxyl groups on the skin surface, ensuring the adhesion of hydrogel to skin. In contrast, in a cool environment, the hydrogen bonds reform to reduce active groups in the PPG hydrogel, leading to viscosity loss and easy removal.

Characterization of the PPG hydrogel

To evaluate the obtained PPG hydrogel, hydrogels with varied component contents (denoted by PVA, PG, PPG₁, PPG₂, and PPG₃) were prepared (Supplementary Table 1). Fourier transform infrared spectra (FTIR) shown in Fig. 2a exhibited that the characteristic

bands of O–H (approximately 3275 cm⁻¹) in the PPG$_{1–3}$ hydrogel were in good agreement with those of the PVA hydrogel[36], while the vibration band at 995 cm⁻¹ only appeared in the PPG$_{1–3}$ hydrogel due to P–O from PA[37]. The details of the characteristic peaks of O–H, C=C, and P–O bonds were illustrated more clearly in Supplementary Fig. 2. First, the intensity of the broad O–H vibration band weakened with increasing PA content due to the formation of hydrogen bonds between PA and PVA. Second, the C=C peak, a result of the destruction of C–OH and C–H bonds in PVA and the formation of ketones and/or enols, was shifted and enhanced with increasing PA content because PA could form intermolecular hydrogen bonds with PVA to reduce the intramolecular hydrogen bonds in PVA[33]. Third, the characteristic stretching band at approximately 1044 cm⁻¹ was attributed to C–N bonds from Gel, which gradually concealed by the increasing intensity of P–O bonds when the intensity increased along with the increasing PA concentration, in the spectra of the PG, PPG₁, PPG₂, PPG₃, and PVA hydrogels. Since the shift of characteristic peaks is often affected by hydrogen bonding, the FTIR spectra of the PPG hydrogel at 4, 37, and 55 °C and room temperature (RT) were explored as shown in Supplementary Fig. 3. The P–O stretching peak has slightly red-shifted with increasing temperature, which could be attributed to their weakened chemical bond energy of P–O bond by the shift of intramolecular hydrogen bond in PVA to intermolecular hydrogen bond of PVA and PA[38,39].

X-ray diffraction (XRD) was employed to illustrate the influence of the hydrogel formulations on PVA crystallization. As shown in Fig. 2b, the typical PVA crystalline peaks located at 19.95 and 41.11° corresponding to the lattice planes (101) and (102), respectively[40]. The peak strength decreased as the content of PA in PPG$_{1-3}$ hydrogel increased, because the crystallization of PVA molecules was weakened by the strong gelatinization of PA[33,38,41]. Meanwhile, UV–vis spectrum (Fig. 2c) showed the optical transparency of PPG hydrogel was greater than 91%, much higher than that of PG and PVA hydrogel. The insert pictures evidenced the highest transmittance of PPG hydrogel. The above results indicate that the weaken crystallization of PVA contributes to the increased transmittance of hydrogel.

The cooperation of hydrogen and ionic bonds endows the PPG hydrogel with good adhesive, self-adaptive, and self-healing properties[33,42], which imply that the PPG hydrogel as sensor patch would stick well on skin and adapt to body movement for continuous data acquisition. As shown in Fig. 2d, the PPG hydrogel pretreated at 55 °C exhibited adhesive behavior on pigskin and a load-bearing capacity of approximately 100 g, indicating appropriate adhesiveness to skin. More interestingly, we found that the pretreated PPG hydrogel showed good adhesive capacity to various materials (Supplementary Fig. 4), including animal tissue (kidney, liver, lung, and spleen), plastic, glass, rubber, and copper, etc. From Fig. 2e, the preheated PPG hydrogel was observed to flow through a syringe tube under gravity at 37 °C, indicating its good self-adaptive property which would prevent contact lost between the hydrogel and skin in motion and avoid the interface impedance increasing. The self-healing property of PPG hydrogel was revealed by optical microscopy images in Fig. 2f. The pretreated PPG hydrogel was cut into halves, and the approximately 200 μm gap between them disappeared within 5 min at 50 °C, reflecting the good self-healing property of the PPG hydrogel. Rheological properties were employed to characterize the self-healing properties. The strain sweep test of PPG hydrogel (Supplementary Fig. 5) identified that the intersection of G' and G'' was 320%, determining the critical point from the elasticity to the flow dynamics. After that, the strain-induced damage and recovery behavior of the PPG hydrogel were investigated by subsequent step measurements. As shown in Fig. 2g, G' dropped dramatically to G'' and exceeded G'' at a 500% high strain because the hydrogel network was disruption, while G' restored at a 1% low strain due to the reversible network rebuilt. These destruction and recovery properties were alternately repeated for more than three cycles, confirming the good self-healing ability of the PPG hydrogel.

Hydrogels, composed of crosslinked polymer networks and water molecules, has great potential in wearable applications with the skin-moduli-matching mechanics and the conductive structure based on mobile ions and mobile electrons. The ionically conductive hydrogels enable design of soft wearable devices mimicking biological systems by using ions rather than electrons as signal carriers for sensing and information processing[43,44]. The 3D microporous structure of hydrogel ion-conductive adhesive plays an important role in its electrical properties and breathability. As shown in Supplementary Fig. 6, PPG hydrogel consisted of a typical microporous structure with a pore size of approximately 1 μm. Such uniform micropores would protect the hydrogel network from collapse to improve its stability and provide more space for the free shuttling of H$^+$ in the channel[45]. Moreover, the connected 3D microporous structure facilitated the exchange of water vapor. From Fig. 2h, PPG hydrogel exhibited a water vapor transmittance ratio (WVTR) of approximately 220 g m^{-2} d^{-1}, which was close to skin breathability (~200 g m^{-2} d^{-1})[46] and better than that of commercial polyurethane (PU) film (3 M Co., 165 g m^{-2} d^{-1}). Water evaporation is a key limiting issue for hydrogel materials which affects device performance[43]. As shown in Fig. 2i, because of bonding between

free water and glycerol, the PPG hydrogel could reduce water evaporation and retain 60% of its original weight while the PVA hydrogel could only retain 10% of its original weight, after storing for 7 days under constant temperature (37 °C) and humidity (60%) conditions. The PPG hydrogel as skin adhesive with good breathability and water retention could prevent users from feeling discomfort, promising good application potential in sensor tape patches for skin.

Biocompatibility of the PPG hydrogel

Since biocompatible hydrogels often provide a suitable environment for bacteria, sticking hydrogels directly on the skin signifies inoculating bacteria on the skin, which poses a potential risk of bacterial infection[47]. Thus, the study of antimicrobial properties in hydrogel materials is essential. The antimicrobial properties of the PPG hydrogel were evaluated using *S. aureus* (gram-positive bacteria) and *E. coli* (gram-negative bacteria) as representative bacteria. As shown in Fig. 3a, an obvious inhibition zones appeared in the PPG hydrogel, with an inhibition diameter of 3.8 cm for *S. aureus* and 4.5 cm for *E. coli*. The inhibition ratios obtained by the co-culturing PPG hydrogel and bacteria (Fig. 3b) were approximately 92.13 ± 0.22 and $94.40 \pm 0.32\%$ for *S. aureus* and *E. coli*, respectively, further indicating that the PPG hydrogel had good antimicrobial properties. Minimum inhibitory concentration (MIC) of PPG hydrogel was performed against *E. coli* and *S. aureus* on 96 well microplate treated. As shown in Supplementary Fig. 7, MIC$_{50}$ values of PPG hydrogel leachates were approximately 8 mg mL^{-1}, for *S. aureus* and *E. coli*. In comparison to PVA and PG hydrogels in Fig. 3a, b, the good antibacterial ability of PPG hydrogel implied that PA played a crucial role in antimicrobial activity. The antibacterial mechanism of the PPG hydrogel was further explored with scanning electron microscopy (SEM) measurement to observe the morphology of bacterial cell walls. As shown in Supplementary Fig. 8, the surface of *E. coli* was obviously damaged and even the bacterial cell wall disintegrated with prolonged co-culture time with the PPG hydrogel. Owing to the strong ability to chelate metal ions and proteins, PA could act to the bacterial cell wall, leading to suppressed cell wall synthesis, cell membrane damage, and massive bacterial death[48]. Thus, the PPG hydrogel rich in PA exhibits good antimicrobial effect.

Pigskin, because of its biological similarity to the human dermis, was employed to examine the interfacial interactions between the PPG hydrogel and biological skin. To imitate practical application in a moist environment, artificial sweat was painted on the surface of pigskin, and fluorescein sodium (FS) dye was added to the PPG hydrogel to facilitate imaging[49]. As shown in Fig. 3c, the hydrogel on the pigskin (left) showed strong fluorescence, while only weak fluorescence remained on the pigskin surface after removal of the hydrogel (right) and the residual amount of FS was approximately 91 μg m^{-2}. As well, the fluorescence was only observable on the surface of the skin (Fig. 3c), indicating that the adhesive effect between the PPG hydrogel and skin existed at the interface. Also, the skin barrier could prevent the ingredients in the hydrogel from penetrating the skin, thereby avoiding discomfort caused by irritation of the skin tissue. To evaluate skin irritation, a skin patch of the PPG hydrogel was bonded to the back of Sprague–Dawley (SD) rats. As shown in Fig. 3d, the skin morphology of the rat back adhered with the PPG hydrogel for 24 h was as normal as that without hydrogel, and no stimulating response (such as erythema or edema) was observed on the skin surface. Moreover, the skin tissues were observed with hematoxylin and eosin (H&E) staining. Figure 3d showed the resulting images of tightly connected collagen fibers, continuous and complete epidermal layer, evenly distributed hair follicles, and no infiltration of inflammatory cells. The histological analysis further proved that the PPG hydrogel skin patch is a nonirritant for skin tissue, laying a fundamental basis for further human skin patch applications. Accordingly, the PPG
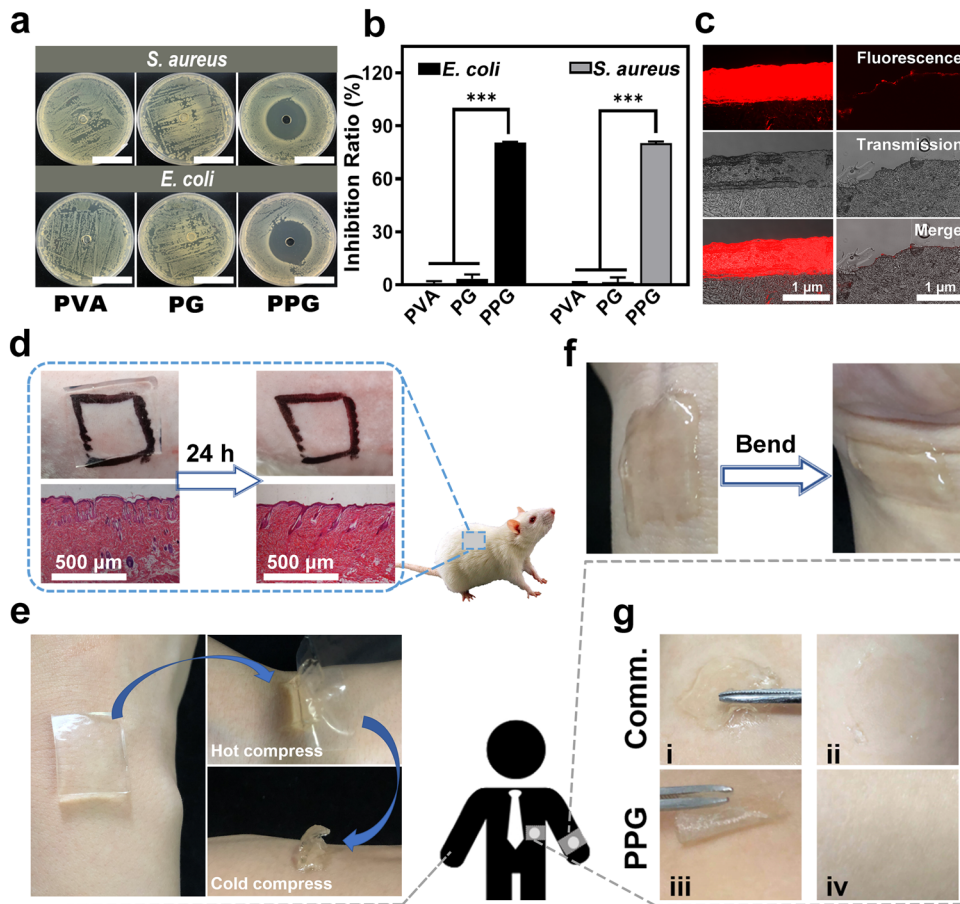
Fig. 3 Biocompatibility of PPG hydrogel. a, b Inhibition zones and inhibition ratios of hydrogels to *E. coli* and *S. aureus* (scale bar: 2 cm, $P^{***} < 0.001$). Error bars represent the standard deviation ($n = 3$). **c** Fluorescence intensity of fluorescence-labeled PPG hydrogel (left) and residual hydrogel (right) on pigskin. **d** Photograph and H&E staining of PPG hydrogel bonded on the back skin of SD rats before and after 24 h. **e** Photographs of PPG hydrogel adhering to and peeling off from skin. **f** Adaptive ability of PPG hydrogel to skin. **g** Photographs of commercial hydrogel (i, ii) and PPG hydrogel (iii, iv) peeled off from the human skin after adhering for 24 h.

hydrogel was applied to the skin of volunteers. As shown in Fig. 3e, the PPG hydrogel exhibited good adhesion after a hot compress and could be easily peeled off with a cool compress. Benefit the suitable temperature window between 4 and 50, the skin would not suffer scalding or frostbite when hot/cold compress. When used on the wrist of volunteers (Fig. 3f), the PPG hydrogel showed good adhesion and adaptability during wrist stretching and bending, indicating that the PPG hydrogel as an electrode could prevent high bioelectrical impedance caused by gaps with curved skin. Subsequently, the PPG hydrogel was applied to volunteers' arms for 24 h to evaluate its suitability as an adhesive patch to skin. Compared with the commercial hydrogel, the PPG hydrogel displayed a distinct advantage in skin patches; that is, it could easily peel off the skin without any residue or irritation (Fig. 3g).

Conductivity and Sensor Properties of the PPG Hydrogel

Under a certain voltage, lots of free hydrogen ions (H^+) ionized by PA could cause directional migration through the hydrogel network, giving an intrinsic conductivity without introducing any extrinsic conductor to hydrogels[38,48]. The conductivity of the PPG hydrogel was $0.13\ s\ m^{-1}$ which could close the circuit and allow the current to flow across. When hydrogel and light-emitting diode (LED) were connected to a closed circuit, the on/off status of the LED lights could directly reflect the conductivity of the hydrogel. As shown in Fig. 4a, the LED was lighted successfully when supplying voltage of circuit is about 5 V, demonstrating the

circuit was closed and PPG hydrogel as a conductor could facilitate the current to flow across. The self-healing property of PPG hydrogel could effectively restore the broken hydrogels and keep the equipment running properly. As shown in Fig. 4b, the lighted LED was goes out with cutting the hydrogel to open the circuit, while would be turned on after re-joining the two halves back and repairing their gaps (circuit scheme in Supplementary Fig. 9). Supplementary Video 1 vividly shows the self-healing ability of PPG hydrogel in the circuit. When two halves hydrogel are connected and heated with a hair dryer (hot and cold air circulation for 3 min), the healed hydrogel can withstand tension and keep the circuit smooth. Pasting the hydrogel on a soft substrate (circuit scheme in Supplementary Fig. 10) and twisting it, the LED light is not affected (Fig. 4c and Supplementary Video 2) because the adhesiveness and self-adaptability of PPG hydrogel could keep the current flow across.

To evaluate its sensitivity and response, the PPG hydrogel as a wearable sensor was attach on the finger joint of volunteers (Fig. 4d) to collected the electrophysiological signal. As shown in Fig. 4e, the resistance of the PPG hydrogel exhibited a clear change when the finger was bent from a straightened state to different angles (45° and 90°), and could restore its original levels when gradually returning the finger to the straightened state. Afterwards, the resistance value changed regularly under the continuous bending of the finger (Fig. 4f), indicating the electrophysiological signals could be obtained in real-time. In addition, more subtle changes in electrical resistance from weak
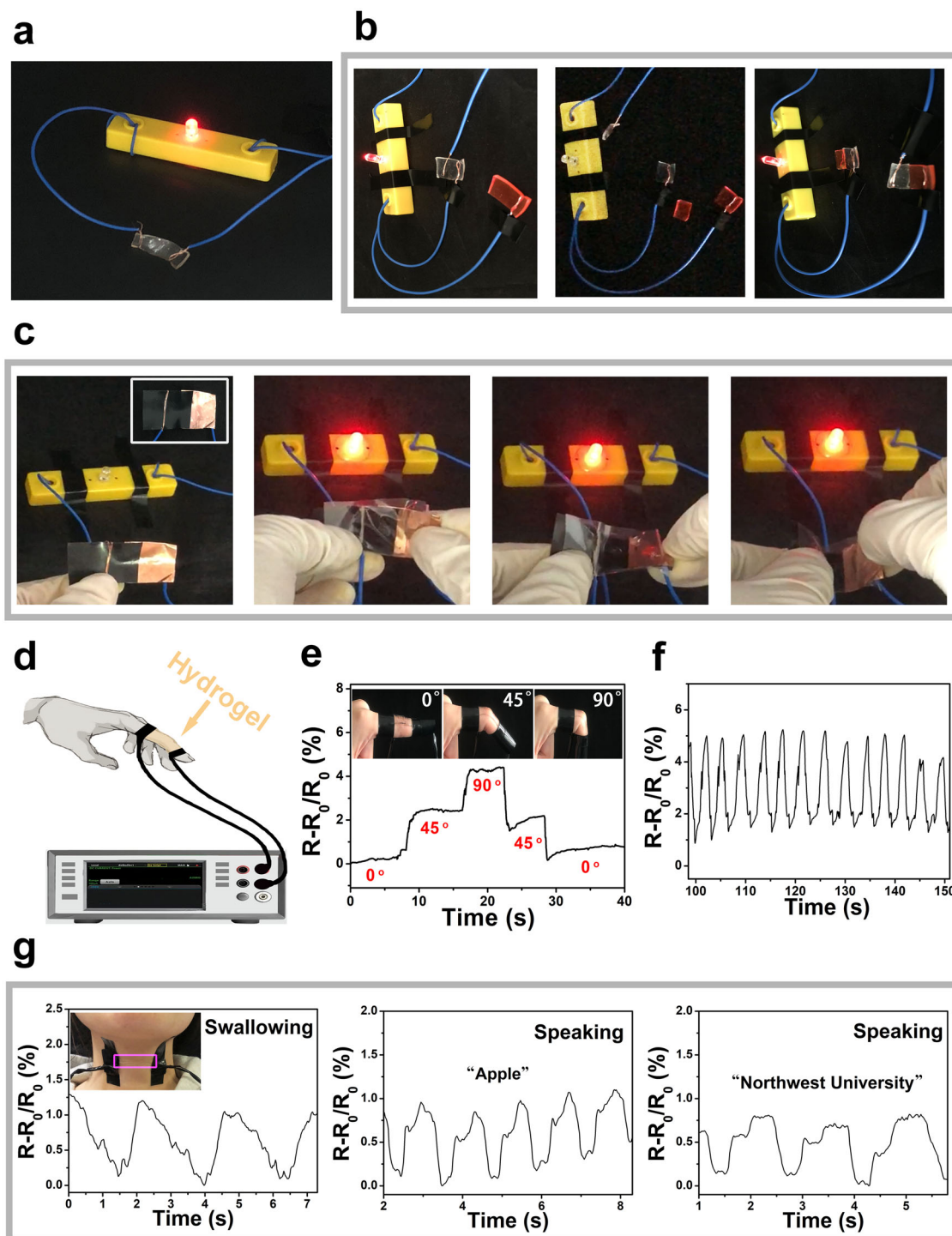
Fig. 4 Electrical properties of PPG hydrogel. a Digital photo of PPG hydrogel in a circuit with LED light. **b, c** Digital photos of self-healing and self-adaptive property of PPG hydrogel in a circuit. (Details of substrate inserted in **c**) **d** Schematic illustration for finger sensing. **e, f** Relative resistance changes of the PPG hydrogel upon bending finger at different angles and bending finger several times in a row. **g** Relative resistance changes of the PPG hydrogel upon swallowing and speaking. (Digital photos of PPG hydrogel as sensor attached on finger and throat inserted in **e** and **g**).

strains were detected at the throat (Fig. 4g). The changes in resistance caused by swallowing could be clearly distinguished, indicating that the PPG hydrogel could record information on throat movement. The tiny yet complicated muscle movements involved in speaking can also be recorded; for example, the relative resistance curve with time when the volunteer pronounced different phrases such as "apple" and "Northwest

University" had a distinct and repeatable characteristic signal. Hence, the PPG hydrogel-based sensor shows high sensitivity and fast response, satisfying the demands of human monitor.

Currently, real-time monitoring of human physiological indicators have become increasingly significant in the diagnosis and prevention of some complex chronic or acute diseases[17,50]. Monitoring the heart is an important part in health monitoring,

but traditional measurements usually require cumbersome and/or expensive external auxiliary device. Due to good ionic conductivity and self-adaptability, PPG hydrogel electrode could form a good contact with skin to reduce interface impedance. As shown in Supplementary Fig. 11, the skin interfacial impedance of PPG hydrogel was 14.5 KΩ at 1 KHz which was lower than that of commercail gel (18.6 KΩ), indicating the performance of PPG hydrogel electrode was similar to commercial gel in electrophysiological signal monitoring. PPG hydrogel as temperature-responsive hydrogel was also placed at different temperatures to detect their interfacial impedance (Supplementary Fig. 12). Although increasing the temperature leads to a decrease in impedance, the impedance is relatively close between 35 and 45 °C. Thus, it is considered that ECG signals from human body would not influence by temperature for our body is remains at 36.5 °C which provide a relatively stable environment for hydrogels. Here, we have assembled a portable sensor (Supplementary Fig. 13, working voltage is 3.5–5.5 V) based on the PPG hydrogel to track human electrophysiological signals in real-time via Bluetooth component, and the regular heartbeats signals were output clearly without any cumbersome appendage equipment. The sensor was attached to the chest with PPG hydrogel as shown in Fig. 5a. When serving as electrodes for ECG diagnosis, the PPG hydrogel showed the same precision and stability as commercial gel electrodes (Fig. 5b). As clearly shown in Fig. 5c, the characteristic peaks (P, Q, R, S, and T waves) collected by the PPG hydrogel were consistent well with the standard signals. Compared with a commercial paster, the PPG hydrogel also featured adaptive ability and tight adhesion to human skin, which favored recording valid signals and continuously diagnosing health status in real-time. As shown in Fig. 5d, when used to monitor heartbeats, the transmitted signals were stable while the volunteer was resting, walking, and breathing deeply, indicating the PPG hydrogel electrode for ECG was reliable. Furthermore, the PPG hydrogel could record the ECG signals clearly after 6, 24, and 48 h (Supplementary Fig. 14), as well as after being repasted 5, 10, and 15 times (Fig. 5e). The results reflect that the PPG hydrogel can be used during long-term wear.
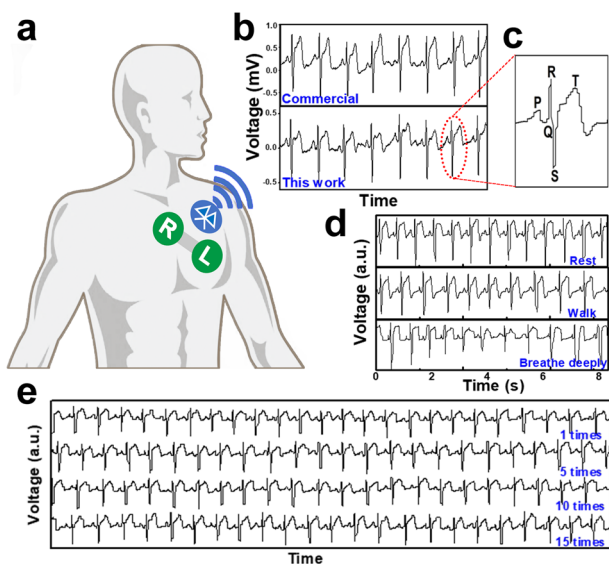

Fig. 5 PPG hydrogel as sensor patch for ECG detection. a Schematic illustration monitoring ECG signals with portable sensor and transmitting via Bluetooth. **b** ECG signals collected from the PPG hydrogel and a commercial hydrogel. **c** Characteristic peaks of ECG collected by PPG hydrogel. **d, e** ECG signals collected with different behaviors and repeated paste times.

Remolding property of the PPG hydrogel
Material recycling not only paves the way for cost savings, but also offers a huge opportunity to reduce waste emissions[51]. Remolding ability is an important and intriguing feature of hydrogels because recycle the waste PPG hydrogel in production could effectively reduce electronic waste and manufacturing cost[52]. Crosslinking with noncovalent interactions, the PPG hydrogel can be recycled without compromising its original performance. When the temperature was increased from 20 to 80 °C, rheological analysis of the PPG hydrogel (Supplementary Fig. 15) showed that the liquefying point was 67 °C, which meant that almost all the crosslinking sites were broken after heating above 67 °C. Thus, the remodeling process of PPG hydrogel was carried out as depicted Supplementary Fig. 16a. First, the scraps of the PPG hydrogel in the production process were collected and cut into fragments, which were placed at 80 °C to destroy the crosslinking sites and obtain liquid mixture. Then, the above mixture could be written or poured into molds to obtain desired shapes. Finally, a reshaped PPG hydrogel was formed after freezing at −20 °C. It is worth noting that the reshaped PPG (re-PPG) hydrogel could maintain its original functions to conduct electricity to make LED light (Supplementary Fig. 16b). As well, the temperature-response viscosity of the re-PPG hydrogel was verified by the rheological properties, and the results matched well with the PPG hydrogel when the temperature was changed from −20 to 60 °C and returned to −20 °C (Supplementary Fig. 17). Afterwards, ECG signals could be effectively collected by re-PPG hydrogel electrodes in Supplementary Fig. 18.

In summary, inspired by the temperature reversibility of hydrogen bonding, a PPG hydrogel with multiple hydrogen bonds was designed for skin-friendly adhesion and health monitoring. The adhesion of PPG hydrogel could be triggered via a hot compress and stably attached to skin to detect electrophysiological signals with low motion artifacts, while a cool compress (around an ice pack temperature) would easily remove it without skin damage. As a safe and comfortable skin patch, the PPG hydrogel constructed with biocompatible PVA and PA exhibited good transparency, breathability, water retention, and antimicrobial activity. Additionally, the self-adaptation, self-healing and conductivity effectively prevented high bioelectrical impedance between the hydrogel and skin, rendering the PPG hydrogel to collect electrophysiological signals during movements. When used as electrodes for ECG diagnostics, the PPG hydrogel could be used repeatedly, as well as deliver stable electrophysiological signals while the volunteer was resting, walking, and breathing deeply. In addition, the PPG hydrogel exhibited good remolding and reusability, which allowed the scraps to be reused and thus satisfied environmental protection needs. Thus, PPG hydrogel is considered to have good application prospects as a sensor in human health monitoring.

METHODS
Materials
Poly(vinyl alcohol) (PVA, MW 89,000–98,000) and gelatin (Gel, from porcine skin) were purchased from Sigma (St. Louis, MO, USA). Glycerol (GL 99.0%), phytic acid solution (PA, 50 wt.% in H_2O), fluorescein sodium (FS), and rhodamine B (Rh B) were purchased from Shanghai Macklin Biochemical Co., Ltd. All materials were used as received.

Preparation of hydrogels
PPG hydrogel was prepared with a facile two-step strategy. In brief, 0.54 g of PVA and 0.06 g of gelatin were first mixed well, and then 1.5 g of glycerol-water binary solvent (1:4) and 3 g of PA aqueous solution were added to the mixture in turn while stirring. The obtained suspension was transferred into a water bath at 80 °C until the powders dissolved and the suspension became a clear liquid. Finally, the liquid was poured into the mold and transferred to −20 °C for 20 h after cooling to temperature.

The control hydrogel samples were prepared using the same method (Table S1). Dye (Rh B) was added to the system to prepare red PPG hydrogels to conveniently observe the PPG hydrogel.

Physicochemical characterizations

Fourier transform infrared (FTIR) spectra (Thermo Fisher Scientific, Waltham, MA, USA) of the samples were recorded in the range of 400–4000 cm^{-1}. Transmittance spectra of the hydrogels were obtained by using a UV–vis spectrophotometer (UV 2600, Shimadzu, Japan) in the visible light range (300–800 nm). To facilitate freeze-drying, the hydrogel was soaked in deionized (DI) water for 24 h to replace glycerin. The freeze-dried hydrogels were characterized by wide-angle X-ray diffraction (XRD, Smart Lab SE) using Cu Kα radiation (λ = 1.54056 Å) in the 2θ range of 5 to 50° with a scan rate of 5° min^{-1}. Scanning electron microscopy (SEM, Carl Zeiss, Oberkochen, Germany) was used to examine the morphologies of freeze-dried hydrogels.

Rheological tests

Rheological characteristics were determined with a rheometer (Anton Paar, MCR302) using a platform with a diameter of 30 mm in oscillation mode. The rheological tests included the following: (1) The variable temperature test was performed with temperature increase and decrease rate of 5 °C min^{-1}, and the temperature was maintained for 5 min at −20, 4, 37, and 60 °C at a fixed strain of 1% and a fixed frequency of 1 Hz. (2) The changes in the storage modulus and the loss modulus were investigated during a strain from 0.1 to 1000% a constant ω of 10 rad s^{-1} at 55 °C. (3) The self-healing properties were investigated with the storage modulus and the loss modulus alternated by changing the oscillating strain amplitudes from 1 to 500% every 200 s at a constant ω of 10 rad s^{-1} at 55 °C.

Breathability

Polyurethane (PU) film was purchased from Minnesota Mining and Manufacturing (3 M) Co. USA. The PPG hydrogel and PU film were complete covered on a cup of water with a diameter of approximately 15 mm, respectively, then placed in a chamber at a constant temperature of 37 °C and humidity of 60%. The control group was placed without any covers. The weight of cup and water was recorded after 24 h, and the water vapor transmission ratio (WVTR) was calculated with Eq. (1).

$$WVTR(\%) = \frac{w_{initial} - w_{24h}}{w_{initial}} \times 100\% \tag{1}$$

Water retention

The hydrogels were placed under constant temperature (37 °C) and relative humidity (60%). The wet weight of the hydrogel was determined every 24 h. The weight ratio was calculated with Eq. (2).

$$Weight\ ratio(\%) = \frac{w_{hydrogel}}{w_{initial\ hydrogel}} \times 100\% \tag{2}$$

Antibacterial assays

The tests included the following:

(1) The antibacterial activity of hydrogels was assessed against *E. coli* and *S. aureus*. Specifically, *E. coli* and *S. aureus* (10^5 CFU mL^{-1}) were uniformly inoculated onto agar plates and then punched with 8 mm diameter holes. The hydrogels were placed into the prepunched wells, and the diameters of the inhibition zone were measured after incubation at 37 °C for 48 h.

(2) To further investigate the antibacterial ability, *E. coli* and *S. aureus* (10^6 CFU mL^{-1}) were inoculated into Luria–Bertani liquid medium (5 mL) and cocultured with the hydrogel (1 g); the blank group was cultured without the hydrogel. Then, the optical density (OD 600) of the bacterial solution over time was recorded after 12 h at 37 °C.

(3) MIC test: Leachates of PPG hydrogel was obtained by immerse the hydrogel in Mueller–Hinton broth medium for 24 h. 100 μL of bacterial suspension (0.1 OD$_{600}$ corresponding 10^8 cells per mL) was placed in each well of a 96-well plate. Then, leachates were diluted and added in 96-well plate to make the final concentration of each well was 20–7 mg mL^{-1}. After cultured at 37 °C for 24 h, the optical density (OD 600) of the bacterial solution was recorded.

The results are expressed as Inhibition% (Eq. (3)), and the tests were repeated three times:

$$Inhibition\ (\%) = \frac{A_{blank} - A_{hydrogel}}{A_{blank}} \times 100\% \tag{3}$$

(4) The morphology of *E. coli* was characterized with SEM. Specifically, *E. coli* was inoculated on a PPG hydrogel and incubated at 37 °C for 1, 2 and 3 h. Then, the hydrogel with *E. coli* was fixed with 4% paraformaldehyde and dehydrated sequentially with 20, 40, 60, 80 and 100% ethanol for approximately 20 min for SEM.

Biocompatibility evaluation

The interfacial interactions between the PPG hydrogel and biological samples were evaluated. Artificial sweat was sprayed onto the surface of thawed pigskin, and then the PPG hydrogel with FS dye (preheated for 5 min at 50 °C) was pasted onto the pigskin. After incubation for 6 h at 37 °C in a humidified chamber, the pigskin was washed with PBS more than 5 times and frozen. The freezing microtome section of that skin was observed and imaged with a fluorescence microscope.

To further evaluate the skin toxicity of the PPG hydrogel, the pretreated PPG hydrogel was applied to the back of depilated SD rats. After 24 h, the rat skin tissues were collected and stained with H&E. The results were observed and imaged with a microscope.

Electrical tests

Digital touchscreen multimeter (Tektronix DMM6500) was employed to measure the electrical properties of the PPG hydrogel. The tests included the following:

(1) The conductivity value was calculated with Eq. (4),

$$\sigma = L/(R \times S) \tag{4}$$

where L is the length, R is the resistance, and S is the contact area of PPG hydrogel.

(2) The sensing measurements of the PPG hydrogel were carried out to monitor human behaviors. Specifically, the 50 °C-preheated hydrogel was adhered to the volunteers' knuckle and throat (the insert photos in Fig. 4e, g), respectively, and then connected to the digital touchscreen multimeter with copper wires. The resistance changes with the volunteers' behaviors were recorded. The resistance change ratio (%) was calculated by Eq. (5),

$$\Delta R/R_0 = (R - R_0)/R_0 \tag{5}$$

where R and R_0 are the resistances with and without strain applied, respectively.

(3) The skin interfacial impedance was measured by an electrochemical workstation (CHI 760) with a range from 1 to 10^6 Hz at 0.03 V. The measurement was carried out by pasting electrodes pairs on forearm skin and keeping a center distance of approximately 5 cm as the insert photo in Supplementary Fig. 11. The interfacial impedance for different temperature was measured by pasting the hydrogel on the pigskin.

(4) The ECG signals while the volunteers walking, deep breathing, and resting were recorded with a Bluetooth acquisition module (BMD 101), and the commercial electrode was Chunfeng (YD-50 Ag/AgCl) gel electrodes.

Statistical analysis

SPSS software was used for statistical analysis and the data were represented as the mean ± standard deviation. Each data was come from at least three independent experiments and one- or two-sided t-test was used to evaluate significant difference between groups. *$p < 0.05$; **$p < 0.01$; ***$p < 0.001$.

DATA AVAILABILITY

All relevant data that support the findings of this study are available from authors upon reasonable request.

REFERENCES

1. Xu, S., Jayaraman, A. & Rogers, J. A. Skin sensors are the future of health care. *Nature* **571**, 319 (2019).
2. Gao, Y., Yu, L., Yeo, J. C. & Lim, C. T. Flexible hybrid sensors for health monitoring: Materials and mechanisms to render wearability. *Adv. Mater.* **32**, 1902133 (2020).
3. Iqbal, S. M. A., Mahgoub, I., Du, E., Leavitt, M. A. & Asghar, W. Advances in healthcare wearable devices. *npj Flex. Electron* **5**, 9 (2021).
4. Han, S. A., Naqi, M., Kim, S. & Kim, J. H. All-day wearable health monitoring system. *EcoMat* **4**, e12198 (2022).
5. Ganesh, R. S., Yoon, H.-J. & Kim, S.-W. Recent trends of biocompatible triboelectric nanogenerators toward self-powered e-skin. *EcoMat* **2**, e12065 (2020).
6. Pan, L. et al. A compliant ionic adhesive electrode with ultralow bioelectronic impedance. *Adv. Mater.* **32**, e2003723 (2020).
7. Yang, C. & Suo, Z. Hydrogel ionotronics. *Nat. Rev. Mater.* **3**, 125–142 (2018).
8. Song, J. et al. Hydrogel-based flexible materials for diabetes diagnosis, treatment, and management. *npj Flex. Electron.* **5**, 26 (2021).
9. Chang, Y. et al. First decade of interfacial iontronic sensing: From droplet sensors to artificial skins. *Adv. Mater.* **33**, 2003464 (2021).
10. Li, G. et al. A stretchable and adhesive ionic conductor based on polyacrylic acid and deep eutectic solvents. *npj Flex. Electron.* **5**, 23 (2021).
11. Cui, N. et al. Stretchable transparent electrodes for conformable wearable organic photovoltaic devices. *npj Flex. Electron* **5**, 31 (2021).
12. Zhang, Y. & Tao, T. H. Skin-friendly electronics for acquiring human physiological signatures. *Adv. Mater.* **31**, e1905767 (2019).
13. Hwang, I. et al. Multifunctional smart skin adhesive patches for advanced health care. *Adv. Healthc. Mater.* **7**, e1800275 (2018).
14. Zhang, Y. S. & Khademhosseini, A. Advances in engineering hydrogels. *Science* **356**, 3627–3639 (2017).
15. Ji, S. et al. Water-resistant conformal hybrid electrodes for aquatic endurable electrocardiographic monitoring. *Adv. Mater.* **32**, e2001496 (2020).
16. Wang, W. et al. Designable micro-/nano-structured smart polymeric materials. *Adv. Mater.* https://doi.org/10.1002/adma.202107877 (2021).
17. Chen, Y. et al. Flexible inorganic bioelectronics. *npj Flex. Electron* **4**, 2 (2020).
18. Yang, J., Bai, R., Chen, B. & Suo, Z. Hydrogel adhesion: A supramolecular synergy of chemistry, topology, and mechanics. *Adv. Funct. Mater.* **30**, 1901693 (2020).
19. Liang, Y., He, J. & Guo, B. Functional hydrogels as wound dressing to enhance wound healing. *ACS Nano* **15**, 12687–12722 (2021).
20. Xie, C., Wang, X., He, H., Ding, Y. & Lu, X. Mussel-inspired hydrogels for self-adhesive bioelectronics. *Adv. Funct. Mater.* **30**, 1909954 (2020).
21. Wang, C., He, K., Li, J. & Chen, X. Conformal electrodes for on-skin digitalization. *SmartMat* **2**, 252–262 (2021).
22. Liang, Y., Li, Z., Huang, Y., Yu, R. & Guo, B. Dual-dynamic-bond cross-linked antibacterial adhesive hydrogel sealants with on-demand removability for post-wound-closure and infected wound healing. *ACS Nano* **15**, 7078–7093 (2021).
23. Xue, Y. et al. Trigger-detachable hydrogel adhesives for bioelectronic interfaces. *Adv. Funct. Mater.* **31**, 2106446 (2021).
24. Baik, S. et al. Bioinspired adhesive architectures: From skin patch to integrated bioelectronics. *Adv. Mater.* **31**, e1803309 (2019).
25. Zhao, X. et al. Physical double-network hydrogel adhesives with rapid shape adaptability, fast self-healing, antioxidant and NIR/pH stimulus-responsiveness for multidrug-resistant bacterial infection and removable wound dressing. *Adv. Funct. Mater.* **30**, 1910748 (2020).
26. Gao, Y., Wu, K. & Suo, Z. Photodetachable adhesion. *Adv. Mater.* **31**, 1806948 (2019).
27. Gao, M. et al. Skin temperature-triggered, debonding-on-demand sticker for a self-powered mechanosensitive communication system. *Matter* **4**, 1962–1974 (2021).
28. Shi, X. & Wu, P. A smart patch with on-demand detachable adhesion for bioelectronics. *Small* **17**, e2101220 (2021).
29. Xu, L. et al. A solvent-exchange strategy to regulate noncovalent interactions for strong and antiswelling hydrogels. *Adv. Mater.* **32**, 2004579 (2020).
30. Mawad, D. et al. A conducting polymer with enhanced electronic stability applied in cardiac models. *Sci. Adv.* **2**, e1601007 (2016).
31. Zhou, H. et al. Robust and sensitive pressure/strain sensors from solution processable composite hydrogels enhanced by hollow-structured conducting polymers. *Chem. Eng. J.* **403**, 126307 (2021).
32. Feng, Y. et al. Solvent-induced in-situ self-assembly lignin nanoparticles to reinforce conductive nanocomposite organogels as anti-freezing and anti-dehydration flexible strain sensors. *Chem. Eng. J.* **433**, 133202 (2021).
33. Zhang, K. et al. Polymerizable deep eutectic solvent-based mechanically strong and ultra-stretchable conductive elastomers for detecting human motions. *J. Mater. Chem. A* **9**, 4890–4897 (2021).
34. Hu, R., Zhao, J., Wang, Y., Li, Z & Zheng, J. A highly stretchable, self-healing, recyclable, and interfacial adhesion gel: Preparation, characterization, and applications. *Chem. Eng. J.* **360**, 334–341 (2019).
35. Lei, H. & Fan, D. Conductive, adaptive, multifunctional hydrogel combined with electrical stimulation for deep wound repair. *Chem. Eng. J.* **421**, 129578 (2021).
36. Zhang, S. J. & Yu, H. Q. Radiation-induced degradation of polyvinyl alcohol in aqueous solutions. *Water Res.* **38**, 309–316 (2004).
37. Zhao, Z., Chen, H., Zhang, H., Ma, L. & Wang, Z. Polyacrylamide-phytic acid-polydopamine conducting porous hydrogel for rapid detection and removal of copper (II) ions. *Biosens. Bioelectron.* **91**, 306–312 (2017).
38. Zhang, S. et al. One-step preparation of a highly stretchable, conductive, and transparent poly(vinyl alcohol)–phytic acid hydrogel for casual writing circuits. *ACS Appl. Mater. Interfaces* **11**, 32441–32448 (2019).
39. Wu, S., Shao, Z., Xie, H., Xiang, T. & Zhou, S. Salt-mediated triple shape-memory ionic conductive polyampholyte hydrogel for wearable flexible electronics. *J. Mater. Chem. A* **9**, 1048–1061 (2021).
40. Luo, X. et al. A flexible multifunctional triboelectric nanogenerator based on MXene/PVA hydrogel. *Adv. Funct. Mater.* **31**, 2104928 (2021).
41. Ballabio, M. et al. Band-like charge transport in phytic acid-doped polyaniline thin films. *Adv. Funct. Mater.* **31**, 2105184 (2021).
42. Wang, T. et al. A self-healable, highly stretchable, and solution processable conductive polymer composite for ultrasensitive strain and pressure sensing. *Adv. Funct. Mater.* **28**, 1705551 (2018).
43. Lyu, Q., Gong, S., Yin, J., Dyson, J. M. & Cheng, W. Soft wearable healthcare materials and devices. *Adv. Health. Mater.* **10**, e2100577 (2021).
44. Gong, S. et al. A gold nanowire-integrated soft wearable system for dynamic continuous non-invasive cardiac monitoring. *Biosens. Bioelectron.* **205**, 114072 (2022).
45. Shao, L. et al. Highly sensitive strain sensor based on a stretchable and conductive poly(vinyl alcohol)/phytic acid/NH2-POSS hydrogel with a 3D micro-porous structure. *ACS Appl. Mater. Interfaces* **12**, 26496–26508 (2020).
46. Lei, H., Zhu, C. & Fan, D. Optimization of human-like collagen composite polysaccharide hydrogel dressing preparation using response surface for burn repair. *Carbohydr. Polym.* **239**, 116249 (2020).
47. Lei, H., Zhao, J., Ma, X., Li, H. & Fan, D. Antibacterial dual network hydrogels for sensing and human health monitoring. *Adv. Healthc. Mater.* **10**, 2101089 (2021).
48. Zhang, Q., Liu, X., Zhang, J., Duan, L. & Gao, G. A highly conductive hydrogel driven by phytic acid towards a wearable sensor with freezing and dehydration resistance. *J. Mater. Chem. A* **9**, 22615–22625 (2021).
49. Wang, R. et al. A dual network hydrogel sunscreen based on poly-γ-glutamic acid/tannic acid demonstrates excellent anti-UV, self-recovery, and skin-integration capacities. *ACS Appl. Mater. Interfaces* **11**, 37502–37512 (2019).
50. Gambhir, S. S., Ge, T. J., Vermesh, O., Spitler, R. & Gold, G. E. Continuous health monitoring: An opportunity for precision health. *Sci. Transl. Med.* **13**, eabe5383 (2021).
51. Tao, X., Liao, S. & Wang, Y. Polymer-assisted fully recyclable flexible sensors. *EcoMat* **3**, e12083 (2021).
52. Rahimi, A. & García, J. M. Chemical recycling of waste plastics for new materials production. *Nat. Rev. Chem.* **1**, 0046 (2017).

AUTHOR CONTRIBUTIONS

F.W.H., R.J.X., and W.L. conceived the project. J.F.H. and W.L. designed the experiments. W.L., J.Y.Z., and Z.X.Y. performed experiments. W.L. and R.J.X. drafted the manuscript and J.S.W., F.W.H., J.F.H., and D.D.F. helped to revise the manuscript. F.W.H., J.F.H., and D.D.F. supervised the project. All authors contributed to the analysis of the manuscript.

COMPETING INTERESTS

The authors declare no competing interests.

ADDITIONAL INFORMATION